APPROXIMATE DETERMINATION OF THE CURRENT RMS VALUE OF THE DC LINK CAPACITOR OF SINGLE-PHASE AND THREE-PHASE PWM CONVERTER SYSTEMS

JOHANN W. KOLAR, HANS ERTL, FRANZ C. ZACH
Technical University Vienna, Power Electronics Section,
Gußhausstraße 27, Vienna, AUSTRIA

Phone: (int)43 222 58801-3886 Fax: (int)43 222 5052666

Keywords: DC Voltage Link PWM Rectifier, Local and Global DC Link Capacitor Characteristics.

Abstract

The determination of the capacitance and current carrying ability of the DC link capacitor is an important point for dimensioning of PWM converter systems.

A calculation method is used which is based on local averaging (related to a pulse period). With this one can describe the time-discontinuous behavior of a PWM converter system by time-quasicontinuous system variables which are related to the local mean and rms values. As this paper shows this method allows to describe the dependencies of the global characteristics (which are related to the fundamental period) of the DC link current and of the DC link capacitor current of single-phase and three-phase DC voltage link converters on the system parameters as simple mathematical expressions. These expressions can be used for dimensioning the DC link. In most cases this allows to omit a detailed analysis of the system behavior by digital simulation.

The quality of the approximation is essentially determined by the system pulse rate. As a comparison with digital simulation results shows, this quality is sufficient for dimensioning purposes for medium and high switching frequencies.

1 Introduction

The calculation of the component stress in a DC voltage link PWM converter system usually is performed based on a digital simulation of the stationary or dynamic operating behavior. There the switching status which determines the voltage formation and the transformation of AC side quantities into DC side quantities can be described by the switching functions of the power devices or of the converter bridge legs. By calculating the harmonics of the switching functions this makes possible the determination of all characteristic values for stationary operation via combination and evaluation of theoretically infinite Fourier series ([1],

The authors are very much indebted to the Austrian Fonds zur Förderung der wissenschaftlichen Forschung which supports the work of the Power Electronics Section at their university.

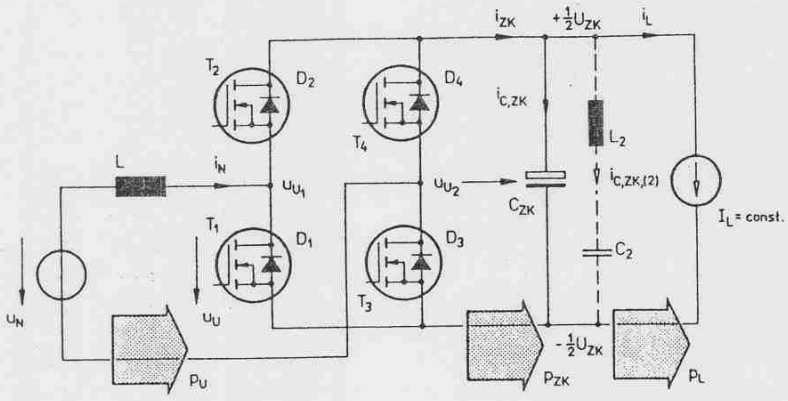

Fig.1: Structure of the power circuit of a single-phase PWM rectifier system (there follows: $p_U(\tau, t_\mu) = p_{ZK}(\tau, t_\mu)$ and $1/T_N \int_{T_N} p_{ZK}(\tau)\, d\tau = 1/T_N \int_{T_N} p_L(\tau)\, d\tau$).

[2], [3], [4]). With this the dimensioning of a PWM converter system is determined by a calculation method which can be easily understood. This concept is, however, very unclear regarding the insight into the "inner" system behavior.

Because this situation is not very satisfactory from a scientific and engineering point of view we have to raise the question of where and when approximate solutions of simple functional structure can be given.

As shown in [5], [6], [7], [8], one can describe the time-discontinuous system behavior of a PWM converter system approximately by time quasi-continuous system variables of corresponding local mean or rms value. There a computation method has to be applied which is based on local averaging, i.e., related to one pulse period. The formulation of the dependencies of the global characteristics (i.e., related to the fundamental period) of the DC link current and the DC link capacitor current of single-phase and three-phase DC voltage link PWM converters on the system parameters then can be performed as simple mathematical expressions. These expressions can be used immediately for dimensioning of the DC link.

The quality of the approximation is essentially determined by the system pulse rate. As a comparison with digital simulation results shows, this quality is sufficient for dimensioning purposes for medium and high switching frequencies as they can be reached with today's turn-off power electronic devices.

The following considerations are performed based on the example of a single-phase and of a three-phase PWM rectifier system. The results obtained can be transferred directly to a PWM inverter system if one interprets the supplying mains and the inductances connected in series as simple equivalent circuit for the fundamental of an AC machine.

2 Single-Phase Four-Quadrant PWM Rectifier System

2.1 General Remarks

As shown in Fig.1, the power circuit of a single-phase bidirectional PWM rectifier system shows the structure of a four-quadrant chopper for operation from the mains. The mains current is defined by the difference between mains and converter voltage occurring across the inductance L connected in series. A proper system control then makes possible an approximately sinusoidal current of selectable phase angle with respect to the mains voltage. The DC link voltage can be controlled by the mains current amplitude; this guarantees the full utilization of the rated power of connected inverter systems, independently of mains voltage variations.

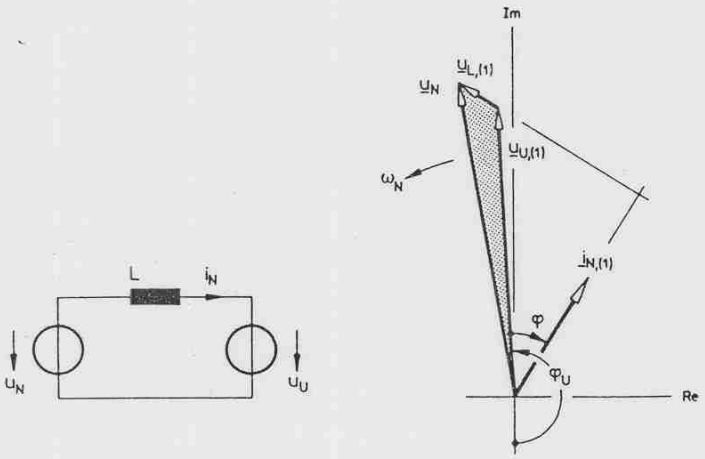

Fig.2: Equivalent circuit of a PWR rectifier system and its description related to the fundamental ($\varphi_U = \omega_N \tau$, $\omega_N = 2\pi/T_N$).

For a mathematical description of the stationary case (which is exclusively related to the fundamental of the system quantities in the following) we can write for the reference values of converter voltage and mains current (using complex AC current calculus)

$$\underline{u}_U^* = \underline{\hat{U}}_U^* \exp j\omega_N t \qquad u_U^* = \Im\{\underline{u}_U^*\} \tag{1}$$

and

$$\underline{i}_N^* = \underline{\hat{I}}_N^* \exp(j\omega_N t + \varphi) \qquad i_N^* = \Im\{\underline{i}_N^*\} \ . \tag{2}$$

The mains current phase angle φ (related to the converter voltage u_U) also denotes approximately the angle between the mains current and mains voltage phasor; this is true because the AC-side inductance usually has a low reactance factor for systems with high pulse rates. For an exact calculation we have to insert the relationship between mains voltage phase angle (related to the mains current) and converter voltage phase angle. This relationship is dependent on the modulation depth, the mains voltage and the value of the inductance. For the sake of brevity we do not want to treat this in more detail in the following because high pulse rates are assumed.

For the equivalent circuit of the AC side of the system there follows Fig.2. In general, the system function is described by

$$L\frac{di_N}{dt} = (u_N - u_U) \ . \tag{3}$$

For the stationary operation there follows with Eqs.(1, 2) and

$$L\frac{di_N^*}{dt} = (u_N - u_U^*) \tag{4}$$

for the converter voltage reference value which has to be generated as mean value for one pulse period

$$u_U^*(\tau) = u_N(\tau) - L\frac{di_N^*}{dt}\Big|_{t=\tau} \ . \tag{5}$$

There the variable τ denotes the position of the pulse interval within the mains fundamental period T_N. It can be defined as macroscopic or global time. Equation (5) implies a motion of the mains current reference time phasor within the pulse period T_P considered according to

$$i_N^*(\tau + t_\mu) = i_N^*(\tau) + \frac{di_N^*}{dt}\Big|_{t=\tau} t_\mu \tag{6}$$

(this means a motion along the tangent which can be given at time τ for the circular trajectory described by the tip of the time phasor of the mains current reference value). The variable t_μ in general is the basis

for describing the microscopic or local time behavior of the system quantities within a pulse interval T_P. With the definition of the deviation

$$\Delta i_N = i_N - i_N^* \tag{7}$$

between the actual mains current and its reference value and combining Eqs.(7, 3 and 4) there follows

$$\frac{d\Delta i_N}{dt_\mu} = \frac{1}{L}\left[u_U^*(\tau) - u_U(\tau, t_\mu)\right] . \tag{8}$$

Equation (8) gives the relationship of the current harmonics (resulting due to the discontinuous operation of the system) in the time domain. Due to the equivalence of local reference value and of local mean value of the actually generated converter voltage

$$u_U^*(\tau) = \frac{1}{T_P}\int_0^{T_P} u_U(\tau, t_\mu)\, dt_\mu \tag{9}$$

we have furthermore

$$\Delta i_N\Big|_{t_\mu = 0, T_P} = 0 . \tag{10}$$

Due to the limitation of the considerations to the fundamentals (denoted by indices (1)) and to the macroscopic time behavior of the system quantities according to

$$u_U(\tau) = u_{U,(1)}(\tau) = u_U^*(\tau) \qquad \text{and} \qquad i_N(\tau) = i_{N,(1)}(\tau) = i_N^*(\tau) \tag{11}$$

we also have

$$\hat{U}_U = \hat{U}_{U,(1)} = \hat{U}_U^* \qquad \text{and} \qquad \hat{I}_N = \hat{I}_{N,(1)} = \hat{I}_N^* . \tag{12}$$

Basically, besides the voltage formation also the transformation or "switching" of the AC side quantities into DC side quantities is defined by the system control. This control has to be set therefore such that the AC side harmonics as well as the stress on the DC link capacitor by DC link harmonics are minimized. The relationships for *unipolar* and *bipolar* control of a four-quadrant chopper are summarized briefly in the following.

2.2 Voltage Formation

The formation of the output voltage of a four-quadrant chopper for antisymmetric control of the bridge legs

$$u_{U_2}(\tau) = -u_{U_1}(\tau) \tag{13}$$

is described by the relationship

$$m(\tau) = 2\alpha_1(\tau) - 1 \qquad m(\tau) = \frac{u_U(\tau)}{U_{ZK}} \tag{14}$$

together with

$$\frac{2u_{U_1}(\tau)}{U_{ZK}} = 2\alpha_1(\tau) - 1 \qquad \frac{2u_{U_2}(\tau)}{U_{ZK}} = 2\alpha_2(\tau) - 1 \qquad \alpha_1 + \alpha_2 = 1 \tag{15}$$

and

$$u_U(\tau) = u_{U_1}(\tau) - u_{U_2}(\tau) . \tag{16}$$

α_1 and α_2 denote the turn-on times of the power devices T2 and T4 (cf. Fig.1) related to the pulse period. For sinusoidal control

$$u_U(\tau) = \hat{U}_U \sin\omega_N\tau \tag{17}$$

we have furthermore

$$\alpha_1(\tau) = \frac{1}{2} + \frac{M}{2}\sin\omega_N\tau \qquad M = \frac{\hat{U}_U}{U_{ZK}} . \tag{18}$$

We have to note that in Eq.(18) the amplitude $\hat{U}_U$ of the generated converter output voltage u_U (the "line-to-line" voltage generated as difference of the phase voltages u_{U_1} and u_{U_2} related to the ficticious DC link voltage center point) is related to U_{ZK} and not to $U_{ZK}/2$. This is done in order to obtain the usual variation of the modulation depth in the region $M \in [0, 1]$.

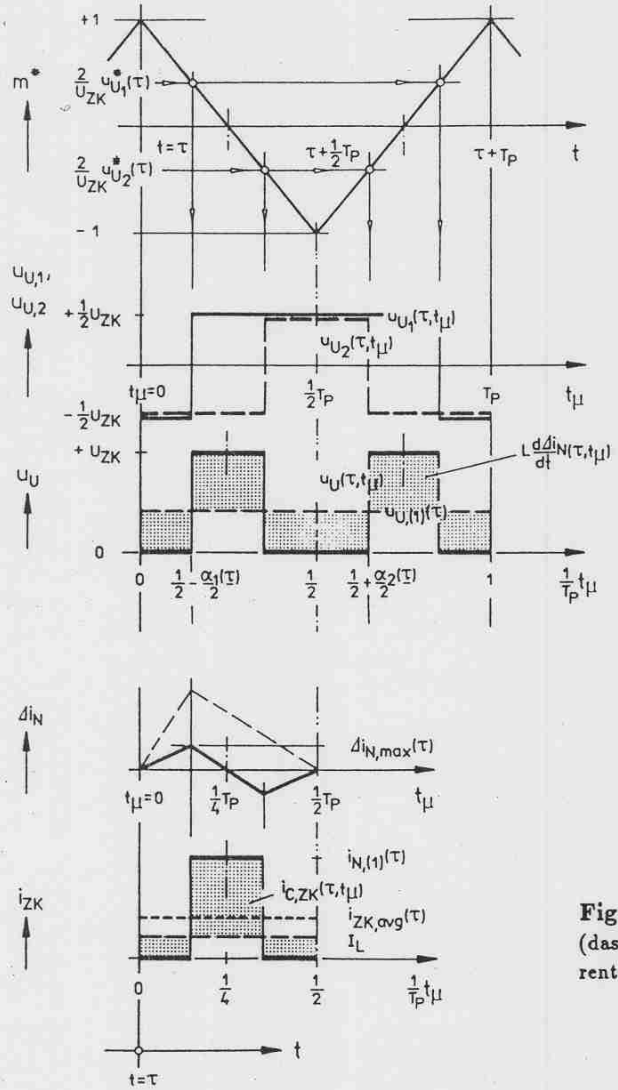

Fig.3: Voltage formation of a single-phase PWM rectifier system for unipolar control.

Fig.4: Unipolar control: mains current ripple (dashed line – bipolar control) and DC link current shape.

2.2.1 Unipolar Control

As Fig.3 shows, the derivation of the control signals of the power devices can be performed in the simplest way by intersection of a triangular signal (with pulse frequency) with the converter output voltage reference value $u^*_U(\tau)$. According to the antisymmetric control mentioned there follow the voltage shapes shown in Fig.3. Within one (local) pulse period there results only one converter output voltage polarity which is defined by the reference value polarity (*unipolar control*). For the maximum deviation of the mains current

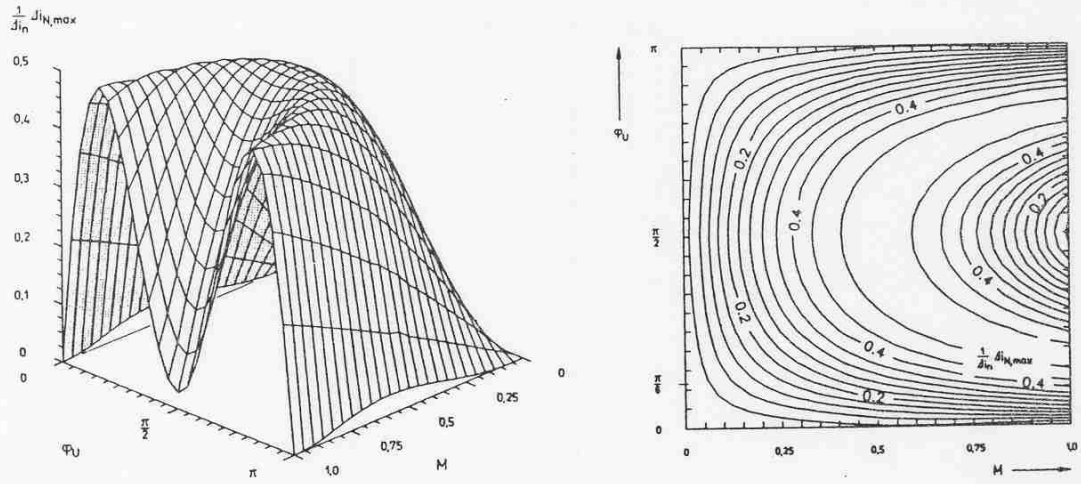

Fig.5: Unipolar control: maximum deviation $\Delta i_{N,max}(\tau)$ in dependency on the modulation index M and on the position τ of the pulse interval.

within one pulse period (local amplitude of the current ripple) there follows with Fig.4 or with

$$\Delta i_N\big|_{t_\mu=0,\,\frac{T_P}{4}} = 0 \tag{19}$$

immediately

$$\Delta i_{N,max}(\tau) = \frac{U_{ZK}T_P}{4L}\left[2-2\alpha_1(\tau)\right]\left[2\alpha_1(\tau)-1\right] \qquad \alpha_1 \geq \alpha_2\,. \tag{20}$$

For sinusoidal control we have furthermore

$$\frac{1}{\Delta i_n}\Delta i_{N,max}(\tau) = 2M\sin\omega_N\tau\,(1-M\sin\omega_N\tau) \qquad \Delta i_n = \frac{U_{ZK}T_P}{8L}\,. \tag{21}$$

For the sake of brevity the description is limited to the angle interval $\varphi_U = \omega_N\tau \in [0,\pi]$. The relationships for other converter voltage angles follow from simple symmetry considerations. Equation (21), shown graphically in Fig.5, can be applied for dimensioning of the AC side inductance L. Furthermore, this relationship makes possible a simple way of estimating the resulting harmonic losses. The local deviation $\Delta i_N(\tau,t_\mu)$ considering the assumed high system pulse rate is transfered into a time function

$$\Delta i^2_{N,rms}(\tau) = \frac{1}{T_P}\int_{T_P}\Delta i^2_N(\tau,t_\mu)\,dt_\mu = \frac{1}{3}\,\Delta i^2_{N,max}(\tau) \tag{22}$$

being quasi-continuous relative to the macroscopic time τ and having equal local power loss. Then there follows, due to the orthogonality between current fundamental and current harmonics, for the approximation of the rms value of the current harmonics

$$\Delta I^2_{N,rms} = \frac{1}{T_N}\int_{T_N}\Delta i^2_{N,rms}(\tau)\,d\tau \tag{23}$$

and

$$\boxed{\frac{1}{\Delta i_n^2}\Delta I^2_{N,rms} = \frac{2}{3}M^2\left(1-\frac{16M}{3\pi}+\frac{3M^2}{4}\right)}\,. \tag{24}$$

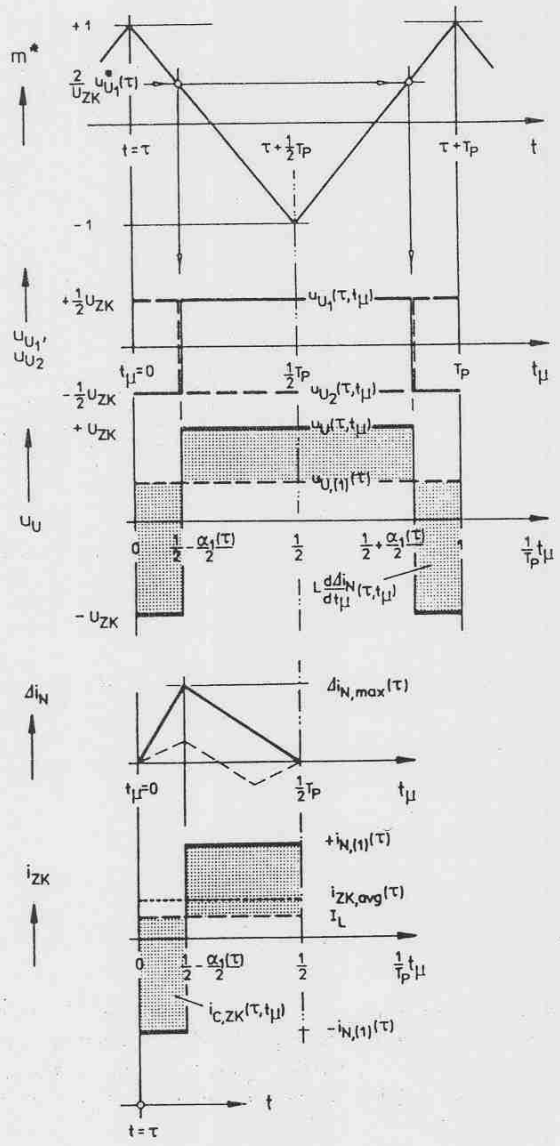

Fig.6: Voltage formation of a single-phase PWM rectifier system for bipolar control.

Fig.7: Bipolar control: mains current ripple (dashed line – unipolar control) and DC link current shape.

2.2.2 Bipolar Control

Contrary to the unipolar control for the especially simple realizable bipolar control the non-voltage-forming switching states (free-wheeling states) of the system are not used. The control of the PWM converter bridge legs is performed according to

$$u_{U_2}(\tau, t_\mu) = -u_{U_1}(\tau, t_\mu) \tag{25}$$

(cf. also Fig.6). Furthermore, Eq.(13) holds again. Independently of the converter output voltage reference value in any case there occur both converter voltage polarities (*bipolar control*).

For the maximum deviation of the mains current within one pulse period there follows with Fig.7

$$\Delta i_{N,max}(\tau) = \frac{U_{ZK} T_P}{L} \alpha_1(\tau) \left[1 - \alpha_1(\tau)\right] \qquad 0.5 \leq \alpha_1 \leq 1 \tag{26}$$

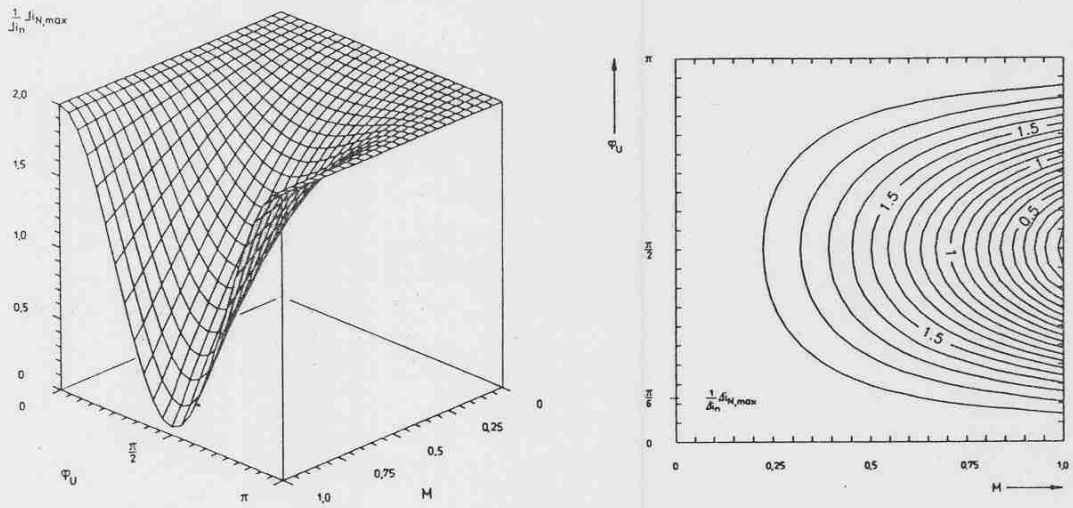

Fig.8: Bipolar control: maximum deviation $\Delta i_{N,max}(\tau)$ in dependency on the modulation index M and of the position τ of the pulse interval.

(positive half wave of the converter output voltage). Furthermore, we have with Eq.(18)

$$\frac{1}{\Delta i_n}\Delta i_{N,max}(\tau) = 2\left(1 - M^2 \sin^2 \omega_N \tau\right) \tag{27}$$

and

$$\boxed{\frac{1}{\Delta i_n^2}\Delta I_{N,rms}^2 = \frac{4}{3}\left(1 - M^2 + \frac{3M^4}{8}\right)}. \tag{28}$$

As a comparison of Figs.5 and 8 and also of Fig.9 shows, the simple bipolar control therefore shows major disadvantages as compared to unipolar converter control. Due to the "ineconomical" voltage formation the mains current harmonics show substantially higher values. This is especially true for the lower modulation region; voltage $u_U = 0$ is obtained by applying of opposite voltage polarities and not by the free-wheeling state as in unipolar control. Furthermore, also the stress on the DC link capacitor is influenced substantially; this will be shown later.

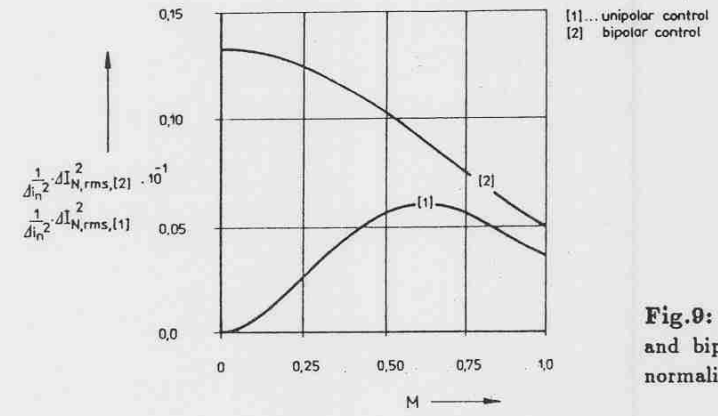

Fig.9: Comparison of unipolar control and bipolar control – comparison of the normalized harmonic power losses.

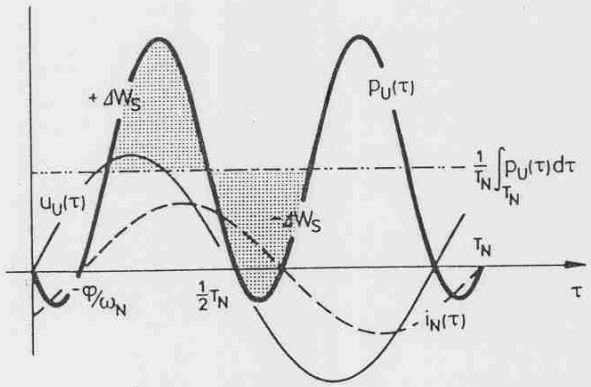

Fig.10: Time dependency of the instantaneous power of a single-phase, purely sinusoidal current-voltage system.

In general unipolar control (as opposed to bipolar control) leads to a doubling of the effective pulse number. In connection with that, it also leads to a corresponding reduction of the harmonics of the system quantities.

Before a more detailed calculation of the DC link current characteristic values is performed, we will briefly discuss the dimensioning of the DC side energy storing device concerning the amount of energy to be stored temporarily. This device is basically required due to the not time-constant power flow in single-phase systems.

2.3 Storage Device Dimension

According to Fig.10 or to

$$p_U(\tau) = u_U(\tau)\, i_N(\tau) = \frac{\hat{U}_U \hat{I}_N}{2} \cos\varphi - \frac{\hat{U}_U \hat{I}_N}{2} \cos(2\omega_N \tau + \varphi)\ , \tag{29}$$

a sinusoidal single-phase voltage/current-system shows a not time-constant power flow, as opposed to three-phase systems. Therefore, the application of an energy storing device becomes necessary (which is formed by a DC link capacitor here) for ideal (constant) load DC current and constant DC link voltage (which results in a constant system output power). There the storage device dimension C_{ZK} has to be determined via the maximum allowable deviation bandwith $\Delta U_{C,ZK}$ of the DC link voltage (and given rated value $U_{ZK,0}$ of the DC link voltage) according to the relationship

$$\Delta U_{C,ZK} \approx \frac{1}{C_{ZK} U_{ZK,0}} \Delta W_S \tag{30}$$

and

$$\Delta W_S = \frac{1}{\omega_N} S_{U,(1)} \qquad S_{U,(1)} = \frac{\hat{U}_U \hat{I}_N}{2} = U_{U,rms} I_{N,rms} \tag{31}$$

or

$$\boxed{\frac{1}{W_n} \Delta W_S = \frac{1}{\pi \cos\varphi}} \tag{32}$$

with

$$W_n = P_{U,(1)} \frac{T_N}{2} \qquad P_{U,(1)} = S_{U,(1)} \cos\varphi\ , \tag{33}$$

respectively. For a simple estimate we can apply the "specific energy storage capability"

$$\Delta w_S = \frac{1}{S_{U,(1)}} \Delta W_S \approx 3.2 Ws/\text{kVA} . \tag{34}$$

The energy to be stored does not constitute the only guideline for determing the size of the DC link capacitor, however; the DC link capacitor in most cases is realized as series/parallel connection of electrolytic capacitors. Due to the very much decreased life time of electrolytic capacitors for operation above the rated temperature[1] the current carrying ability is linked immediately to the equivalent series resistance (ESR) and to the cup size and/or to the value of the capacitance.

In the following we therefore want to discuss the calculation of the capacitor current rms value which determines the thermal stress. There we have to consider the frequency dependency of the ESR for electrolytic capacitors. (The ESR decreases for increasing frequency.) In order to consequently pursue the approximation method and for an estimate of an upper limit we really only can link the capacitor current rms value (which is determined by *all* DC link current harmonics) to *one* single frequency. Therefore, as follows from considerations described later, for unipolar control (cf. Fig.4) we have to take the ESR value for twice the pulse frequency ($f_P = 1/T_P$), for bipolar control (cf. Fig.7) the ESR value for the pulse frequency.

2.4 Characteristic Values of the DC Link Current

Due to the discontinuous operation (dependent on the converter switching state) segments of the mains current are transferred into the DC link within each pulse period. The stress on the DC link capacitor is given by current contributions with pulse frequency. Their amplitude is essentially linked to the instantaneous value of the mains current fundamental. The mains current harmonics (which can be influenced by the pulse frequency) for higher output power (in the rated working point) have only a minor influence on the DC link capacitor current rms value. This is because their amplitude is low, related to the current fundamental amplitude. This clearly justifies the neglection of the mains current harmonics for the approximate calculation of the DC link capacitor current, as performed here.

2.4.1 Unipolar Control

According to Fig.1 we have for the capacitor current

$$i_{C,ZK} = i_{ZK} - i_L . \tag{35}$$

For the local DC link current rms value there follows with Fig.4 in general

$$i^2_{ZK,rms}(\tau) = i^2_N(\tau)\,[2\alpha_1(\tau) - 1] = i^2_N(\tau)\, m(\tau) \tag{36}$$

or, for sinusoidal control

$$i^2_{ZK,rms}(\tau) = M \sin\omega_N\tau \; i^2_N(\tau) . \tag{37}$$

The global DC link current rms value becomes

$$\boxed{I^2_{ZK,rms} = \frac{2M}{3\pi}\hat{I}^2_N(1 + \cos^2\varphi)} \tag{38}$$

(cf. also Fig.11). For the local DC link current mean value we have

$$i_{ZK,avg}(\tau) = M\frac{1}{2}\hat{I}_N\left[\cos\varphi - \cos(2\omega_N\tau + \varphi)\right] . \tag{39}$$

[1] One has to keep in mind that an increase of 10^0C of the capacitor core above the rated temperature will cut the capacitor life time in about one half.

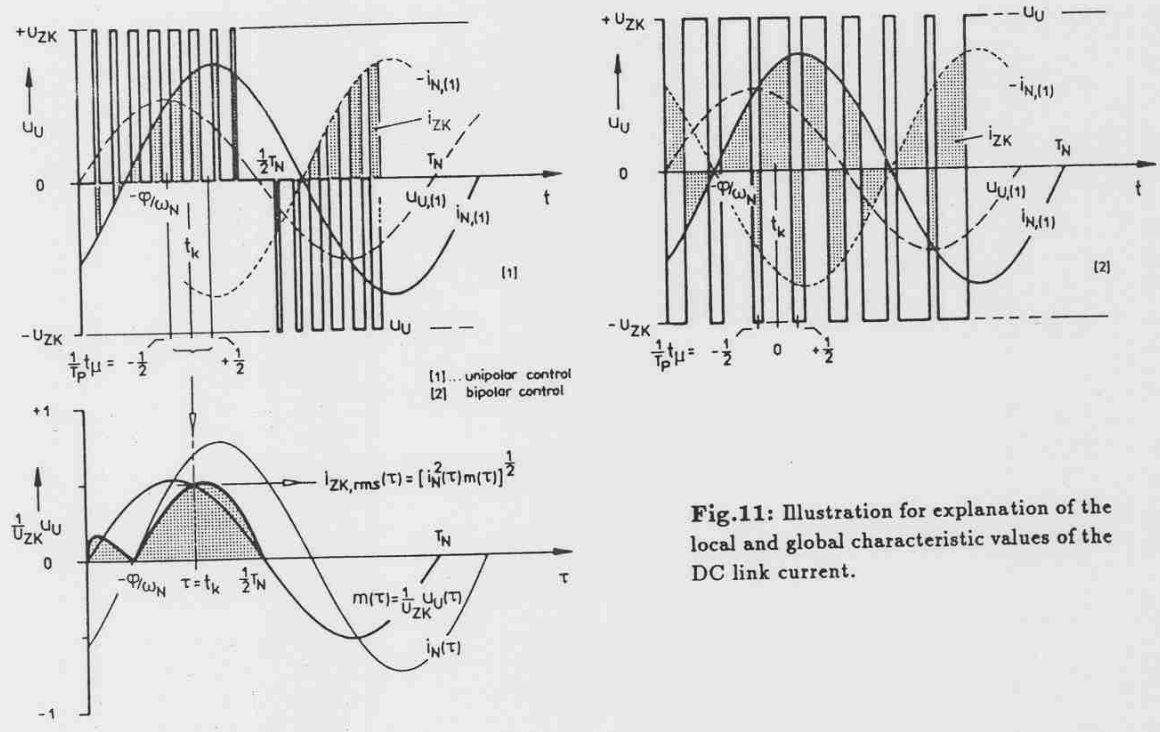

Fig.11: Illustration for explanation of the local and global characteristic values of the DC link current.

It shows an AC contribution according to the instantaneous system power which oscillates with twice the mains frequency. The global mean value of the DC link current shall be set as (time-constant) load current

$$i_L = I_L = \frac{1}{2} M \hat{I}_N \cos\varphi \ . \tag{40}$$

With the relationships

$$i_L = i_{ZK} - i_{C,ZK} \ , \tag{41}$$

$$I^2_{ZK,rms} = \frac{1}{T_N} \int_{T_N} \left[i_{C,ZK}(\tau) + i_L(\tau) \right]^2 d\tau \ , \tag{42}$$

$$\int_{T_N} i_L(\tau)\, i_{C,ZK}(\tau)\, d\tau = 0 \qquad i_L(\tau) = I_L = \text{const.} \ , \tag{43}$$

or

$$I^2_{C,ZK,rms} = I^2_{ZK,rms} - I^2_L \ , \tag{44}$$

respectively, there follows for the rms value of the DC link capacitor current

$$\boxed{I^2_{C,ZK,rms} = M \hat{I}^2_N \left[\frac{2}{3\pi} + \cos^2\varphi \left(\frac{2}{3\pi} - \frac{M}{4} \right) \right]} \tag{45}$$

(cf. also Fig.12).

If the capacitor current component having twice the mains frequency

$$I_{C,ZK,(2),rms} = \frac{1}{2\sqrt{2}} M \hat{I}_N \tag{46}$$

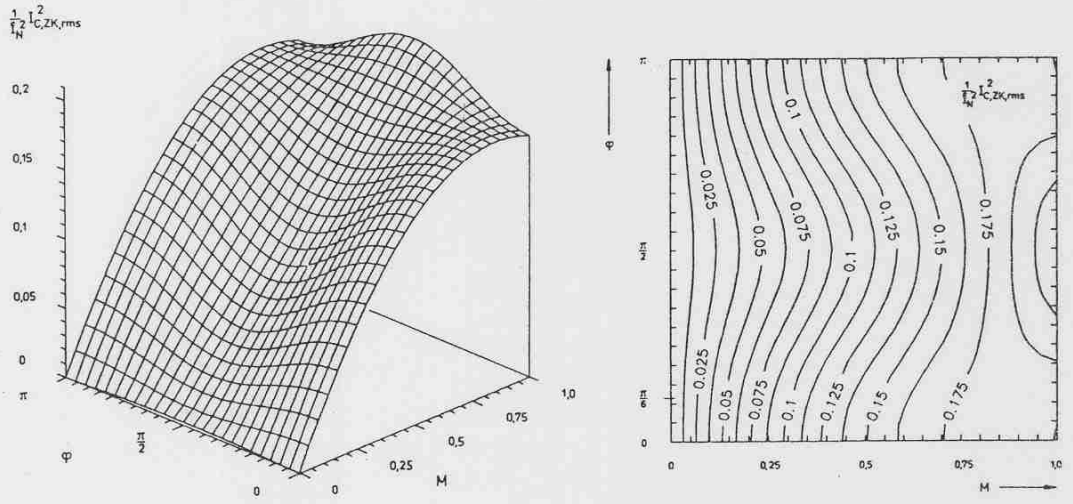

Fig.12: Unipolar control: dependency of the squared DC link capacitor current rms value on the modulation index M and on the phase relationship φ between converter output voltage and mains current fundamental.

is decoupled by a proper tuned series resonant circuit (L_2, C_2) lying in parallel to the DC link capacitor (cf. Fig.1), there remains for the capacitor current stress

$$I^2_{C,ZK,LC,rms} = I^2_{C,ZK,rms} - I^2_{C,ZK,(2),rms} \tag{47}$$

or

$$\boxed{M\hat{I}^2_N \left[\left(\frac{2}{3\pi} - \frac{M}{8} \right) + \cos^2\varphi \left(\frac{2}{3\pi} - \frac{M}{4} \right) \right]}, \tag{48}$$

respectively.

2.4.2 Bipolar Control

As treated before for unipolar control we can derive for bipolar control considering Fig.7

$$i^2_{ZK,rms}(\tau) = i^2_N(\tau) \tag{49}$$

and

$$I^2_{ZK,rms} = \frac{1}{2}\hat{I}^2_N \tag{50}$$

and finally

$$\boxed{I^2_{C,ZK,rms} = \hat{I}^2_N \left(\frac{1}{2} - \frac{M^2}{4}\cos^2\varphi \right)} \tag{51}$$

(cf. also Fig.13). The comparison of the capacitor stress for unipolar and bipolar control (cf. Fig.12 and Fig.13 rotated by 180^0) again shows the advantage of unipolar control compared with bipolar control (cf. section 2.2). According to the voltage formation shown in Fig.6, for bipolar control also for converter output voltage $u_U(\tau) = 0$ an AC current with pulse frequency is switched into the DC link. In contrary, in this case for unipolar control there exists no coupling between AC side and DC side ($i_{ZK}(\tau, t_\mu) = 0$).

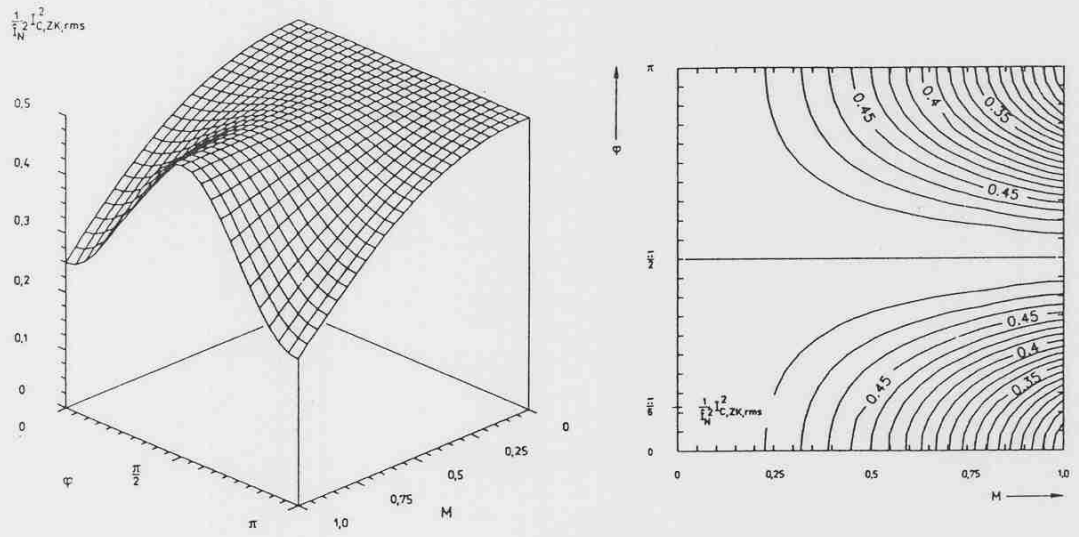

Fig.13: Bipolar control: dependency of the squared DC link capacitor current rms value on the modulation index M and on the phase relationship φ between converter output voltage and mains current fundamental.

3 Single-Phase Four-Quadrant DC Machine Drive

The considerations performed so far have been limited to a constant system output current. If, as shown in Fig.14, the mains converter is applied to supply the DC link of a four-quadrant machine converter there results a drive system of especially high quality. It shows low torque ripple and low influence of the mains, besides high dynamics. The DC link capacitor is loaded by the DC link current contributions of both PWM converters, however.

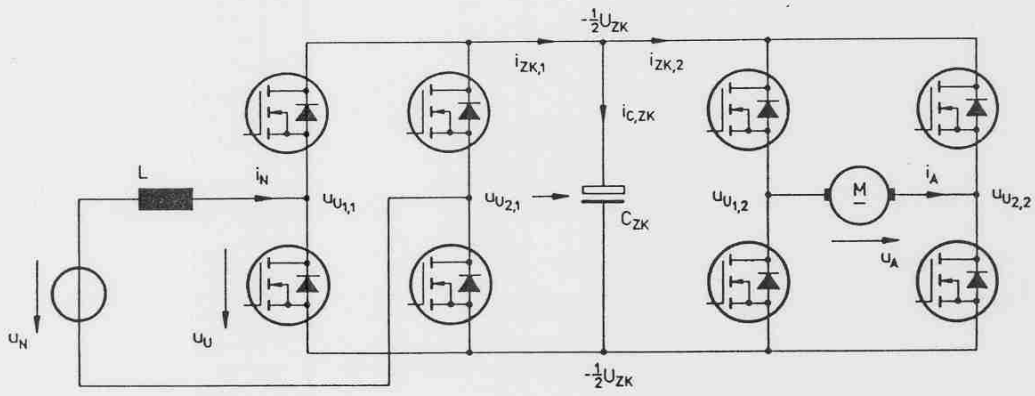

Fig.14: Structure of the power circuit of a single-phase four-quadrant DC machine drive.

For the voltage formation of the converter systems we have with

$$\begin{aligned} \alpha_{1,1} + \alpha_{2,1} &= 1 \\ \alpha_{1,2} + \alpha_{2,2} &= 1 \end{aligned} \qquad (52)$$

for the local mean values of the converter voltages

$$\begin{aligned} u_U(\tau) &= U_{ZK}\left[2\alpha_{1,1}(\tau)-1\right] \\ u_A(\tau) &= U_{ZK}\left[2\alpha_{1,2}(\tau)-1\right] . \end{aligned} \tag{53}$$

The local mean values of the DC link currents follow as

$$\begin{aligned} i_{ZK,1,avg}(\tau) &= i_N(\tau)\left[2\alpha_{1,1}(\tau)-1\right] \\ i_{ZK,2,avg}(\tau) &= i_A(\tau)\left[2\alpha_{1,2}(\tau)-1\right] . \end{aligned} \tag{54}$$

Since we supply a DC machine we have furthermore (for stationary operation)

$$i_A(\tau) = I_A = \text{const.} \tag{55}$$

(where a sufficiently high armature inductance is assumed) and

$$u_{A,avg}(\tau) = U_A = \text{const.} \tag{56}$$

The DC link capacitor current is given by

$$i_{C,ZK} = i_{ZK,1} - i_{ZK,2} , \tag{57}$$

using the directions of current shown in Fig.14. For the global capacitor current rms value, considering the CAUCHY-SCHWARZ inequality

$$\left[\int_{T_N} i_{ZK,1,rms}(\tau)\; i_{ZK,2,rms}(\tau)\; d\tau\right]^2 \le \left[\int_{T_N} i^2_{ZK,1,rms}(\tau)\; d\tau\right] + \left[\int_{T_N} i^2_{ZK,2,rms}(\tau)\; d\tau\right] , \tag{58}$$

in general

$$I_{C,ZK,rms} \le I_{ZK,1,rms} + I_{ZK,2,rms} \tag{59}$$

can be derived in a simple way. The maximum thermal stress on the DC link capacitor (which, as mentioned before, essentially influences its life time) occures for completely "uncorrelated" operation of the converter systems (related to the power flows into the DC link). If the control signals of the two PWM converters are gained by intersection of the voltage reference values with the same carrier signal ("synchronization" of the converters), we can easily give the then essentially lower capacitor current rms value using the calculation method presented here. In the following we want to assume a unipolar control of the two systems due to the advantages discussed in sections 2.2 and 2.4. For the modulation depth of the two converters we set

$$M_1 = \frac{\hat{U}_U}{U_{ZK}} \qquad M_2 = \frac{U_A}{U_{ZK}} . \tag{60}$$

According to a global (extended over the mains fundamental period) power balance there follows between mains and armature current

$$\cos\varphi := 1 \qquad I_A = \frac{1}{2}\hat{I}_N \frac{M_1}{M_2} . \tag{61}$$

The desired, as complete as possible, avoidance of the stress on the mains by fundamental reactive power here is introduced by the assumption of $\cos\varphi = 1$. As Fig.15 shows, we have to distinguish the two cases

$$u_U(\tau) \le U_A \quad \text{and} \quad u_U(\tau) > U_A \tag{62}$$

concerning the formation of the capacitor current. For the local mean value of the capacitor current we have for both cases, however,

$$i_{C,ZK,avg}(\tau) = -\frac{1}{2} M_1 \hat{I}_N \cos 2\omega_N \tau . \tag{63}$$

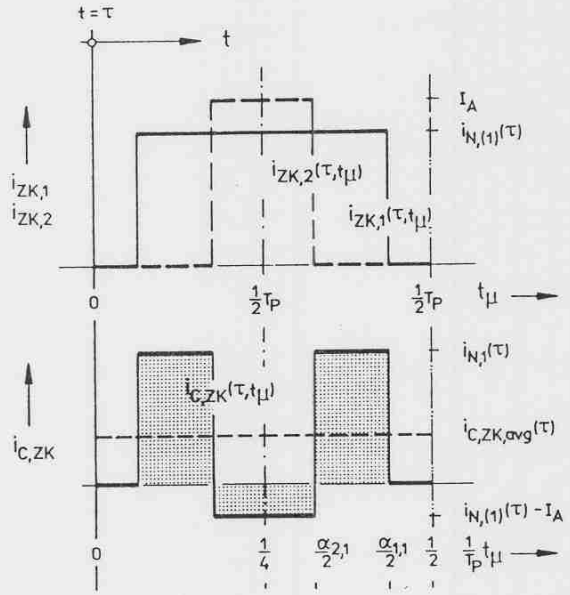

Fig.15: Shape of the DC link currents for $u_U(\tau) \geq U_A$.

This is true because for time-macroscopic consideration there occurs only an energy oscillation of twice the mains frequency due to the constant power flow in the machine converter (cf. section 2.3, Eq.(29)). For the local capacitor current rms value we have in the region $u_U(\tau) \leq u_A$

$$i^2_{C,ZK,rms}(\tau) = i^2_N(\tau)\frac{u_U(\tau)}{U_{ZK}} + I^2_A\frac{U_A}{U_{ZK}} - 2I_A\, i_N(\tau)\frac{u_U(\tau)}{U_{ZK}} \tag{64}$$

$$i^2_{C,ZK,rms}(\tau) = M_1^2\hat{I}^2_N\left(\frac{1}{4M_2} + \frac{1}{M_1}\sin^3\omega_N\tau - \frac{1}{M_2}\sin^2\omega_N\tau\right) \tag{65}$$

and for $u_U(\tau) \geq U_A$

$$i^2_{C,ZK,rms}(\tau) = i^2_N(\tau)\frac{u_U(\tau)}{U_{ZK}} + I^2_A\frac{U_A}{U_{ZK}} - 2I_A\, i_N(\tau)\frac{u_A(\tau)}{U_{ZK}} \tag{66}$$

$$i^2_{C,ZK,rms}(\tau) = M_1^2\hat{I}^2_N\left(\frac{1}{4M_2} + \frac{1}{M_1}\sin^3\omega_N\tau - \frac{1}{M_1}\sin\omega_N\tau\right)\,. \tag{67}$$

Equation (66) follows from Eq.(64) simply by interchanging the action of the mains converter and of the machine side converter.

The global capacitor current rms values therefore are defined via the relationships

$$I^2_{C,ZK,rms} = \frac{2}{\pi}\int_0^{\pi/2} i^2_{C,ZK,rms}\Big|_{u_U(\tau)\leq U_A} d(\omega_N\tau) \qquad \hat{U}_U \leq U_A \tag{68}$$

or

$$\boxed{I^2_{C,ZK,rms} = M_1\hat{I}^2_N\left(\frac{4}{3\pi} - \frac{1}{4\kappa_{21}}\right)} \qquad \kappa_{21} \geq 1 \tag{69}$$

and

$$I^2_{C,ZK,rms} = \frac{2}{\pi}\left[\int_0^{\varphi_{U,1}} i^2_{C,ZK,rms}\Big|_{u_U(\tau)\leq U_A} d(\omega_N\tau) + \int_{\varphi_{U,1}}^{\pi/2} i^2_{C,ZK,rms}\Big|_{u_U(\tau)>U_A} d(\omega_N\tau)\right] \qquad \hat{U}_U \geq U_A \tag{70}$$

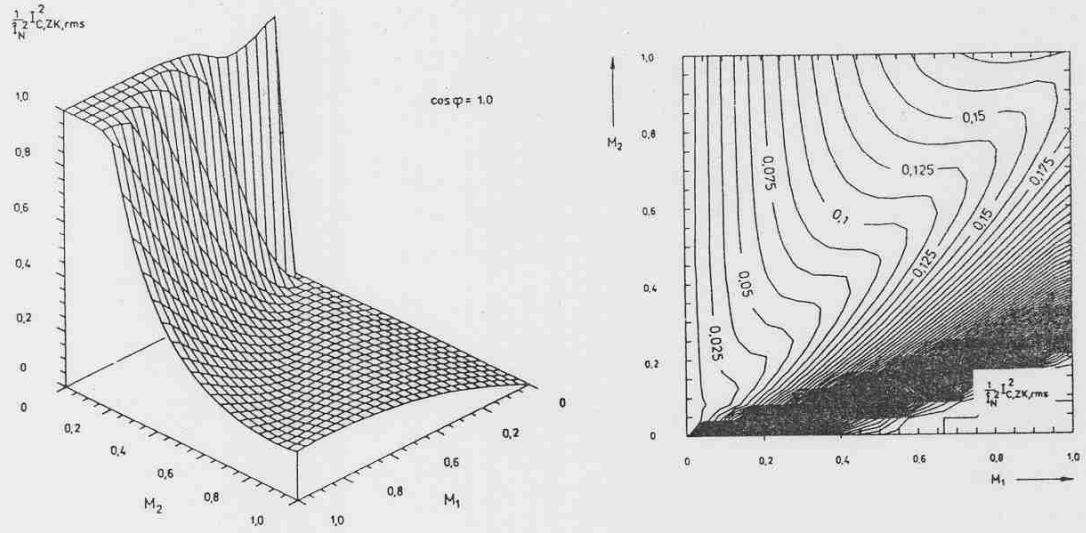

Fig.16: Dependency of the stress on the DC link capacitor on the modulation indices M_1 and M_2 of the mains converter and the machine side converter.

with

$$\varphi_{U,1} = \omega_N \tau_1 = \arcsin \kappa_{21} \ , \qquad u_U(\varphi_1) = U_A \ , \tag{71}$$

or

$$\boxed{I^2_{C,ZK,rms} = M_1 \hat{I}^2_N \left[\frac{4}{3\pi} + \frac{1}{4\kappa_{21}} - \frac{1}{\pi} \left(\sqrt{1-\kappa^2_{21}} + \frac{1}{\kappa_{21}} \arcsin \kappa_{21} \right) \right]} \qquad \kappa_{21} \in [0,1] \ . \tag{72}$$

There κ_{21} denotes according to

$$\kappa_{21} = \frac{M_2}{M_1} \tag{73}$$

the ratio of the modulation indices of the converters.

A comparison of Eqs.(69) and (72) and of the relationship

$$I^2_{C,ZK,rms} \leq M_1 \hat{I}^2_N \left[\frac{4}{3\pi} + \frac{1}{4\kappa_{21}} + 2\sqrt{\frac{1}{3\kappa_{21}}} \right] \tag{74}$$

(which can be obtained by further evaluation of Eq.(59)) clearly shows the influence of the coupling of the control of the two power electronic systems. We have to note, however, that only for bipolar control the worst case can occur, as described for the case of equality in Eq.(74); this can be verified by a more thorough analysis of the capacitor current shapes occurring for free control of the two converters.

The graphic illustration of Eqs.(69) and (72) leads to Fig.16. For the free-wheeling state of the mains converter ($M_1 = 0$) there occurs no DC link power flow and no DC link capacitor current flow. For decreasing modulation index of the machine side converter the stress on the DC link capacitor (which delivers the difference of the instantaneous power of the two converters) rises. This is because then the power flow through the DC link leads to narrow DC link current blocks of high amplitude on the machine side.

4 Three-Phase Four-Quadrant PWM Rectifier System

Besides the characteristic values of single-phase PWM converter systems (as calculated here so far), especially the stress on the DC link capacitor of a three-phase PWM rectifier system (cf. Fig.17) is of special interest; this is especially the case for the realization of PWM converter systems with higher output power. A detailed treatment of this problem is given in [8], based on the calculation method introduced here. Therefore we only want to briefly discuss the essential aspects here.

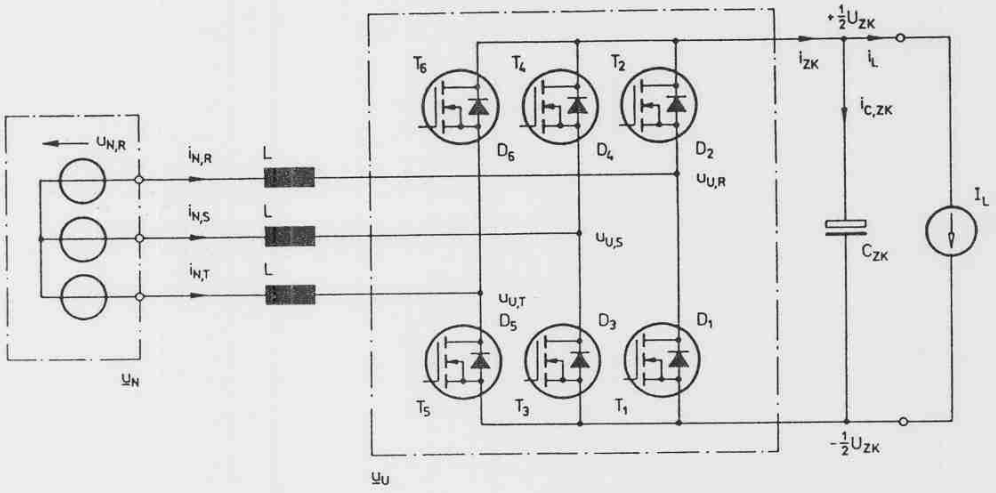

Fig.17: Structure of the power circuit of a three-phase PWM rectifier system.

For the relative turn-on intervals (related to the pulse period) of the power devices T2, T4 and T6 of the upper bridge half (cf. Fig.17) we have in analogy to Eq.(18)

$$\begin{aligned} \alpha_R(\tau) &= \frac{1}{2} + \frac{M}{2}\sin\omega_N\tau \\ \alpha_S(\tau) &= \frac{1}{2} + \frac{M}{2}\sin\left(\omega_N\tau - \frac{2\pi}{3}\right) \\ \alpha_T(\tau) &= \frac{1}{2} + \frac{M}{2}\sin\left(\omega_N\tau + \frac{2\pi}{3}\right) . \end{aligned} \tag{75}$$

The amplitude of the converter voltages (phase voltages) here is related to one half of the DC link voltage according to

$$M = \frac{2\hat{U}_U}{U_{ZK}} \qquad M \in [0; 2/\sqrt{3}] . \tag{76}$$

For the mains current fundamentals we want to set

$$\begin{aligned} i_{N,R}(\tau) &= \hat{I}_N \sin\left(\omega_N\tau + \varphi\right) \\ i_{N,S}(\tau) &= \hat{I}_N \sin\left(\omega_N\tau + \varphi - \frac{2\pi}{3}\right) \\ i_{N,T}(\tau) &= \hat{I}_N \sin\left(\omega_N\tau + \varphi + \frac{2\pi}{3}\right) . \end{aligned} \tag{77}$$

Due to the three-phase property of the system it is completely characterized by consideration of the behavior in the angle interval

$$\varphi_U = \omega_N\tau \in \left[\left(\pi - \frac{\pi}{6}\right), \left(\pi + \frac{\pi}{6}\right)\right] . \tag{78}$$

For the local mean value and the local rms value of the DC link current we then have

$$i_{ZK,avg}(\tau) = -i_{N,T}(\tau)\Big[\alpha_R(\tau) - \alpha_T(\tau)\Big] + i_{N,S}(\tau)\Big[\alpha_S(\tau) - \alpha_R(\tau)\Big] \tag{79}$$

and

$$i^2_{ZK,rms}(\tau) = i^2_{N,T}(\tau)\Big[\alpha_R(\tau) - \alpha_T(\tau)\Big] + i^2_{N,S}(\tau)\Big[\alpha_S(\tau) - \alpha_R(\tau)\Big] \,. \tag{80}$$

The local mean value of the DC link current shows the time-constant value

$$i_{ZK,avg}(\tau) = \frac{3}{4}\hat{I}_N M \cos\varphi = I_{ZK,avg} = I_L \tag{81}$$

for sinusoidal control, contrary to the single-phase system. This is caused by the time-constant instantaneous power of a three-phase purely sinusoidal current-voltage system.

For a theoretically infinitely high switching frequency there now macroscopically is given the equivalence of the local mean value of the DC link current and of a load current assumed constant here. Therefore, the DC link capacitance does not have to meet the requirement of functioning as a (macroscopically acting) energy storage device; a dimensioning guideline corresponding to Eq.(30) does not exist here. However, compared to finite pulse frequency there occurs only a reduction of the current stress on the DC link capacitor by the mains current harmonic contribution (which is neglected here, anyway). This is the case because also for very high pulse rates the mains currents are projected into a discontinuous DC link current.

The dimensioning of the DC link capacitor has to be performed via the capacitor current rms value accordingly. The capacitance value to be selected based on this dimensioning in most cases guarantees a more than als sufficient dimensioning result related to the voltage ripple showing pulse frequency. There low influence of the equivalent series inductance (ESL) and of the equivalent series resistance (ESR) is assumed.

As mentioned before, in the following we set

$$I_L = i_{ZK,avg}(\tau) = const. \tag{82}$$

With

$$I^2_{ZK,rms} = \frac{3}{\pi}\int_{\left(\pi-\frac{\pi}{6}\right)}^{\left(\pi+\frac{\pi}{6}\right)} i^2_{ZK,rms}(\tau)\, d(\omega_N \tau) \tag{83}$$

there follows for the global DC link current rms value

$$\boxed{I^2_{ZK,rms} = \frac{\sqrt{3}}{\pi} M \hat{I}^2_N \left(\frac{1}{4} + \cos^2\varphi\right)} \,. \tag{84}$$

Considering the relationships

$$i_{ZK} = i_{C,ZK} + I_L \tag{85}$$

$$\int_{T_N} I_L\, i_{C,ZK}(\tau)\, d\tau \;=\; 0 \tag{86}$$

we have

$$I^2_{C,ZK,rms} = I^2_{ZK,rms} - I^2_L \tag{87}$$

(cf. Eqs.(41), (42), (43), (44)). For the DC link capacitor current rms value we have herewith

$$\boxed{I^2_{C,ZK,rms} = M \hat{I}^2_N \left[\frac{3}{4\pi} + \cos^2\varphi \left(\frac{\sqrt{3}}{\pi} - \frac{9}{16} M\right)\right]} \,. \tag{88}$$

The graphical illustration of Eq.(88) (cf. Fig.18) shows a pronounced analogy with the result gained for unipolar control of a single-phase system (cf. Fig.12). This is because also here (e.g., for simple subharmonic control) the converter free-wheeling states within each pulse period are included into the voltage formation of the system. The maxima of the DC link capacitor current rms value occurring for modulation depths close to 0.5 can be clearly explained by considering the rms value of the AC component of a unipolar square wave signal with variable duty ratio α (which reaches a maximum for $\alpha = 0.5$).

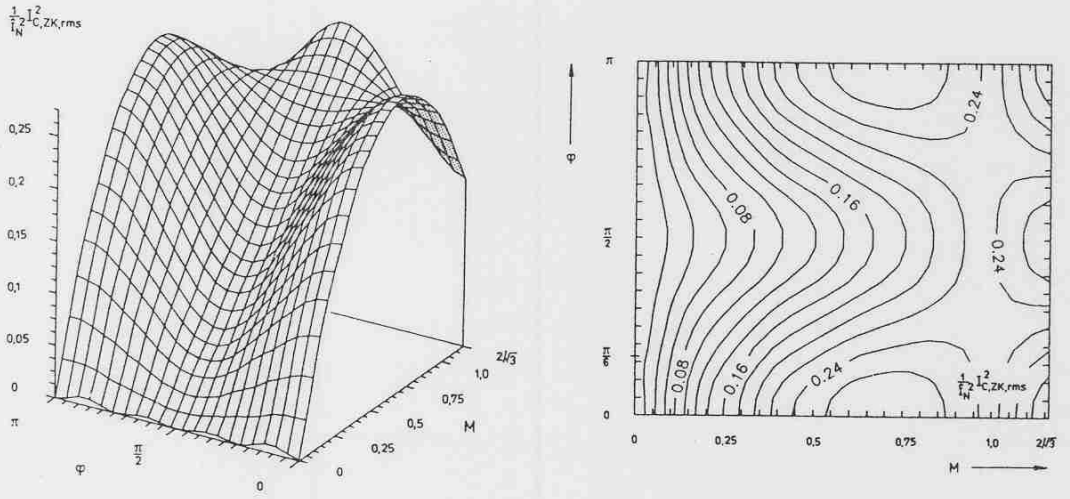

Fig.18: Dependency of the squared DC link capacitor current on the modulation index M and on the phase shift φ between converter phase voltage fundamental and mains current fundamental.

5 Conclusions

Within the scope of this paper we want to omit (for the sake of brevity) a comparison of the calculated approximations with the results of a digital simulation. As shown in [8] for a three-phase PWM converter system, the quality of the approximation for $p_Z = T_P/T_N \geq 21$ in any case is given to such a degree that it is sufficient for dimensioning purposes. Because there do not exist basic differences between single-phase and three-phase systems concerning the formation of the DC link current, we therefore can omit the verification for single phase systems. This is true especially also because the pulse numbers of systems applying modern turn-off power devices (IGBT, FET,...) lie at high values $p_Z \gg 21$; the approximate solution converge for very high pulse numbers in any case to the exact values according to the applied neglections.

In general, the simple mathematical expressions given here can be applied directly for dimensioning the DC link of a PWM converter system. Furthermore, due to the obtained relationships there is made possible a deeper insight into the inner system behavior and a very time-consuming digital simulation can be omitted in many cases.

References

[1] **Rosa, J.:** *The Harmonic Spectrum of DC Link Currents in Inverters.* Proceedings of the 4th PCI Conference, San Francisco, March 29–31, 38–52 (1982).

[2] **Ziogas, P. D., and Photiadis, P.:** *An Exact Input Current Analysis of Ideal Static PWM Inverters.* Conference Record of the 17th IEEE IAS Annual Meeting, San Franciso, Oct. 4–7, 813–822 (1982).

[3] **Ziogas, P. D., Wiechmann, E. P., and Stefanović, V. R.:** *A Computer-Aided Analysis and Design Approach for Static Voltage Source Inverters.* IEEE Transactions on IA, Vol.IA-21, No.5, 1234–1241 (1985).

[4] **Evans, P. D., and Hill-Cottingham, R. J.:** *DC Link Current in PWM Inverters.* IEE Proceedings, Vol.133, Pt.B, No.4, 217–224 (1986).

[5] **Schönung, A., and Brenneisen, J.:** *Bestimmungsgrößen des selbstgeführten Stromrichters in sperrspannungsfreier Schaltung bei Steuerung nach dem Unterschwingungsverfahren.* ETZ-A, Bd.90, H. 14, 353–357 (1969).

[6] **Mall, H. G.:** Application of MP-Capacitors as Input and Filter Capacitors in Transistorized Choppers. Proceedings of the 2nd International Power Conversion Conference, Munich, Sept. 3–5, 3B.6-1–3B.6-7 (1980).

[7] **van der Broeck, H. W.:** *Untersuchung des Oberschwingungsverhaltens eines hochtaktenden Vierquadrantenstellers.* etzArchiv, Bd.8, H.6, 195–199 (1986).

[8] **Kolar, J. W., Ertl, J. and Zach, F. C.:** *Calculation of the Passive and Active Component Stress of Three Phase PWM Converter Systems with High Pulse Rate.* Proceedings of the 3rd European Conference on Power Electronics and Applications, Aachen, Oct. 9–12, Vol.III, 1303–1311 (1989).

In the following there shall be given (without claiming completeness) some further publications where details of dimensioning the DC link of DC voltage link PWM converters are treated:

[9] **Kampschulte, B.:** *Der Einfluß der Energiespeicher im Zwischenkreisumrichter eines Asynchronmaschinenantriebes auf die Oberschwingungen.* Archiv für Elektrotechnik 62, 359–367 (1980).

[10] **Neil J. Barabas:** *Simplified Control Algorithm for Active Power Factor Correction.* Proceedings of the 10th PCI Conference, Chicago, Oct. 22–25, 1–9 (1985).

[11] **Habetler, T. G., and Divan, D.M.:** *Rectifier/Inverter Reactive Component Minimization.* Conference Record of the 22th IEEE IAS Annual Meeting, Atlanta, Oct. 18–23, Pt. I, 648–657 (1987).

[12] **Taufig, J. A., Xiaoping, J., Allan, J., and Burdett, S.:** *A Simple Method of Calculating Inverter DC Side Current Harmonics.* Proceedings of the 3rd European Conference on Power Electronics and Applications, Aachen, Oct. 9–12, Vol.I, 93–97 (1989).

The following publications shall be referenced due to their extensive discussion of generating the DC link current based on AC side currents:

[13] **Boys, J. T.:** *Novel Current Sensor for PWM AC Drives.* IEE Proceedings, Vol.135, Pt.B, No.1, 27–32 (1988).

[14] **Green, T. C., and Williams, B. W.:** *Derivation of Motor Line-Current Waveforms from the DC-Link Current of an Inverter.* IEE Proceedings, Vol.136, Pt.B, No.4, 196–204 (1989).